PHYSICAL REVIEW D **78,** 123528 (2008)

Some cosmological implications of hidden sectors

J. R. Espinosa,[1,*] T. Konstandin,[2,†] J. M. No,[1,‡] and M. Quirós[2,3,4,§]
[1]*IFT-UAM/CSIC, Facultad de Ciencias UAM, E-28049 Madrid, Spain*
[2]*IFAE, Universitat Autònoma de Barcelona, E-08193 Bellaterra, Barcelona, Spain*
[3]*Institució Catalana de Recerca i Estudis Avançats (ICREA), Spain*
[4]*Theory Division, Physics Department, CERN, CH 1211 Geneva 23, Switzerland*
(Received 16 October 2008; published 22 December 2008)

We discuss some cosmological implications of extensions of the standard model with hidden-sector scalars coupled to the Higgs boson. We put special emphasis on the conformal case, in which the electroweak symmetry is broken radiatively with a Higgs mass above the experimental limit. Our refined analysis of the electroweak phase transition in this kind of models strengthens the prediction of a strongly first-order phase transition as required by electroweak baryogenesis. We further study gravitational wave production and the possibility of low-scale inflation as well as a viable dark matter candidate.

DOI: 10.1103/PhysRevD.78.123528 PACS numbers: 98.80.Cq, 95.35.+d

I. INTRODUCTION

The standard model of particle physics (SM) is nowadays considered to be an effective theory valid only up to a certain physical cutoff scale. Even though there exist a large variety of extensions of the SM, models with a hidden sector have recently attracted some attention. We will consider models with additional scalar fields that might transform nontrivially under a hidden gauge group but which are singlets under the SM gauge group. The only renormalizable interaction of such scalars with the SM occurs via the Higgs sector, which in this case serves as a portal to the hidden sector [1].

In this paper we are concerned with some of the possible cosmological implications of hidden-sector extensions of the SM. This is a continuation of the study of the electroweak breaking and phase transition presented in Ref. [2] and we will provide some technical details that were omitted there. In addition we will present an analysis of other cosmological implications, namely, gravitational wave production and dark matter abundance. We also comment on the possibility of low-scale inflation and present a calculation of the bubble wall velocity in the case of a first-order electroweak phase transition. As in Ref. [2] we pay special attention to the classically conformal case which, for a strong coupling between the hidden-sector scalars and the Higgs field, can be consistent with the mass bounds on the Higgs particle.

The paper is organized as follows. In Sec. II, the model is presented, both at zero and finite temperature. In Sec. III the cosmological implications of the model mentioned above are discussed, and we conclude in Sec. IV.

*jose.espinosa@cern.ch
†konstand@ifae.es
‡josemi.no@uam.es
§quiros@ifae.es

II. THE MODEL

A. Zero temperature potential

We consider a set of N_S real scalar fields S_i coupled to the SM Higgs doublet H with the tree-level potential

$$V_0 = m^2 H^\dagger H + \lambda (H^\dagger H)^2 + \sum_i \left(\frac{1}{2} m_{S_i}^2 + \zeta_i^2 H^\dagger H \right) S_i^2. \tag{1}$$

We assume there are no linear or cubic terms in the hidden-sector scalar fields [this can be enforced by some global symmetry, e.g. $O(N)$]. Besides, we assume that the squared masses of the hidden scalars are semipositive definite ($m_{S_i}^2$), such that this global symmetry remains unbroken and no quartic terms are necessary to stabilize the potential.

In the presence of a background Higgs field, $\langle H^0 \rangle = \phi/\sqrt{2}$, the one-loop effective potential in Landau gauge and $\overline{\text{MS}}$ scheme is then given by

$$\begin{aligned} V_{1\text{-loop}} &= V_0 + \Delta V_{1\text{-loop}} \\ &= \frac{m^2}{2}\phi^2 + \frac{\lambda}{4}\phi^4 + \sum_\alpha \frac{N_\alpha M_\alpha^4(\phi)}{64\pi^2} \\ &\quad \times \left[\ln \frac{M_\alpha^2(\phi)}{Q^2} - C_\alpha \right]. \end{aligned} \tag{2}$$

The subscript $\alpha = \{Z, W, t, H, G, S_i\}$ denotes the gauge bosons (Z^0 and $W^\pm$), top quark, Higgs boson, Goldstone bosons (G^0 and $G^\pm$), and hidden-sector scalar fields with $N_\alpha = \{3, 6, -12, 1, 3, N_S\}$ while $C_\alpha = 5/6$ for gauge bosons and $3/2$ for fermions and scalars. The ϕ-dependent tree-level masses are

$$\begin{aligned} M_{S_i}^2(\phi) &= m_{S_i}^2 + \zeta_i^2 \phi^2, \qquad M_Z^2(\phi) = \tfrac{1}{4}(g^2 + g'^2)\phi^2, \\ M_W^2(\phi) &= \tfrac{1}{4} g^2 \phi^2, \end{aligned} \tag{3}$$

$$M_t^2(\phi) = \tfrac{1}{2} y_t^2 \phi^2, \qquad M_H^2(\phi) = 3\lambda\phi^2 + m^2,$$
$$M_G^2(\phi) = \lambda\phi^2 + m^2, \tag{4}$$

where g and g' denote the SM gauge couplings and y_t the top quark Yukawa coupling.

As it was mentioned in the introduction the case with classical conformal invariance (i.e. $m^2 = 0$ and $m_{S_i}^2 = 0$) is especially interesting. In this situation all masses are proportional to the Higgs vacuum expectation value (VEV) and no dimensionful parameters enter into the tree-level potential. However, conformal invariance is broken by loop corrections as can be seen in Eq. (2) by the occurrence of the renormalization scale Q. In this way a mass scale is introduced via dimensional transmutation [2,3]. Notice that an important difference with respect to the pure ϕ^4 theory is that, in the interesting region of the parameter space, the loop contributions are dominated by the hidden-sector scalar (and top) particles. Hence, it is not mandatory to improve the one-loop potential by renormalization group techniques (unlike in the ϕ^4 theory) and moreover the Goldstone and Higgs one-loop contributions to the potential can be safely neglected [3,4]. In the classically conformal case the correct VEV follows from the minimization condition

$$\lambda = -\sum_\alpha \frac{N_\alpha M_\alpha^4(v)}{16\pi^2 v^4}\left[\ln\frac{M_\alpha^2(v)}{Q^2} - C_\alpha + \frac{1}{2}\right], \tag{5}$$

where $v \simeq 246$ GeV is the observed Higgs VEV of the SM and Q should be chosen near v. The potential then reads as

$$V_{\text{1-loop}}^{\text{conf}} = \frac{m_H^2}{8v^2}\phi^4\left[\ln\frac{\phi^2}{v^2} - \frac{1}{2}\right], \tag{6}$$

where m_H is the one-loop Higgs mass given by

$$m_H^2 = \frac{\partial^2}{\partial\phi^2} V\Big|_{\phi=v} = \sum_\alpha \frac{N_\alpha M_\alpha^4(v)}{8\pi^2 v^2}. \tag{7}$$

One can see that the occurrence of a sizable number of hidden-sector scalars, rather strongly coupled to the Higgs field, can lead to a Higgs mass above the LEP bound, even if the theory is classically conformal invariant [5].

Given the fact that the dramatic impact on electroweak symmetry breaking we find is due to a sizable number of scalars somewhat strongly coupled to the Higgs, one might worry about the stability of the results when higher-order corrections to the potential are included. It is straightforward to obtain the dominant two-loop radiative corrections to the Higgs potential (those that depend on the top Yukawa coupling y_t and ζ) by using standard techniques, as e.g. those used in Ref. [6]. We have found that these two-loop effects never modify the structure of the potential in a qualitative way.

Finally, we would like to comment on the influence of the hidden-sector scalars on the cubic Higgs self-coupling. In Ref. [7] the claim was made that a strong phase transition often would lead to a deviation of the cubic Higgs coupling from its SM value. Taking only into account the top and hidden-sector scalar contributions, one obtains

$$\frac{\partial_\phi^3 V}{\partial_\phi^3 V^{\text{SM}}} - 1 = \frac{\sum_i \zeta_i^4}{12\pi^2 M_H^2/v^2 - 3y_t^4}, \tag{8}$$

which will be correlated with the strength of the phase transition in a later section.

B. Finite temperature potential

In order to study the electroweak phase transition of the model, we consider the one-loop potential at finite temperature including the resummed Daisy diagrams. The corresponding contributions are given by

$$\Delta V_T = \frac{T^4}{2\pi^2}\sum_\alpha N_\alpha \int dx\, x^2 \log[1 \pm \exp(-\sqrt{x^2 + M_\alpha^2/T^2})]$$
$$+ \frac{T}{12\pi}\sum_{\alpha\in\text{bosons}} N_\alpha\{M_\alpha^3 - [M_\alpha^2 + \Pi_\alpha(T)]^{3/2}\}, \tag{9}$$

where the $+(-)$ holds for fermions (bosons) and $\Pi_\alpha(T)$ are the thermal masses of the different bosonic species. Neglecting small g' contributions they read

$$\Pi_G = \Pi_H = \left(\frac{1}{2}g^2 + \frac{1}{4}y_t^2 + \frac{1}{2}\lambda + \frac{1}{12}\sum_i \zeta_i^2\right)T^2, \tag{10}$$

$$\Pi_{S_i} = \frac{1}{3}\zeta_i^2 T^2, \qquad \Pi_W = \Pi_Z = \frac{11}{6}g^2 T^2. \tag{11}$$

Besides, in the resummed Daisy diagrams only the longitudinal polarizations of the gauge bosons contribute.

III. COSMOLOGY OF HIDDEN-SECTOR SCALARS

In this section we discuss cosmological implications of the hidden-sector scalar extensions of the SM. Namely, the electroweak phase transition, low-scale inflation, the bubble wall velocity during a first-order phase transition, gravitational wave production, and dark matter are analyzed.

A. Electroweak phase transition

In order to study the electroweak phase transition, we determine the so-called bounce solution of the three-dimensional Euclidean action that quantifies the tunneling probability in the case of a first-order phase transition [8–10].

At finite temperature the bounce solution is obtained by extremizing the action

$$S_3 = 4\pi\int_0^\infty d\rho\,\rho^2\left[\left(\frac{d\phi}{d\rho}\right)^2 + V(\phi)\right], \tag{12}$$

(where ρ is the radial distance from the center of the bubble) with solutions obeying the boundary conditions

$$\partial_\rho \phi(0) = 0, \qquad \lim_{\rho\to\infty} \phi(\rho) = 0. \tag{13}$$

In addition it is understood that the bounce solution ϕ starts (at $\rho = 0$) close to the global minimum of the potential (the broken phase of the Higgs vacuum).

The tunneling rate per unit volume and time element is approximately given by [10]

$$\Gamma \simeq \kappa_3 T^4 \exp[-S_3(T)/T], \tag{14}$$

with $\kappa_3 = [S_3(T)/(2\pi T)]^{3/2}$, such that the average number of bubble nucleations per Hubble volume is given by

$$P(T) = \int_T^{T_c} \kappa_3 \frac{d\tilde{T}}{\tilde{T}} \frac{\tilde{T}^4}{H^4} \exp[-S_3(\tilde{T})/\tilde{T}], \tag{15}$$

where the Hubble parameter is given by

$$H^2 \simeq \frac{8\pi^3 g_* T^4}{90 M_{\rm Pl}^2}, \tag{16}$$

$g_* \simeq 106.75 + N_S$ is the effective number of degrees of freedom and $M_{\rm Pl} = 1.22 \times 10^{19}$ GeV is the Planck mass.

Tunneling becomes, in principle, possible below the temperature T_c at which the two minima of the potential are degenerate, but for almost degenerate vacua, the tunneling rate is still too small to start the phase transition. We define the temperature T_n at which the phase transition starts by the average occurrence of one bubble per Hubble volume

$$P(T_n) = 1. \tag{17}$$

The first nucleation of bubbles will hence approximately take place when

$$\frac{S_3(T_n)}{T_n} \simeq 4\log\left(\frac{T_n}{H}\right) \simeq 142 - 4\log\left(\frac{T_n}{v}\right). \tag{18}$$

In order to characterize the end of the phase transition the fraction of space that is covered by bubbles can be used. Neglecting overlapping bubbles this is given by

$$f(T) = \frac{4\pi}{3} \int_T^{T_c} \kappa_3 \frac{d\tilde{T}}{\tilde{T}} \frac{\tilde{T}^4}{H} R^3(T, \tilde{T}) \exp[-S_3(\tilde{T})/\tilde{T}], \tag{19}$$

where

$$R(T, \tilde{T}) = \frac{v_b}{H}\left(1 - \frac{T}{\tilde{T}}\right). \tag{20}$$

Here $v_b \simeq 1$ is the velocity of the bubble wall and we define the end of the phase transition T_f by

$$f(T_f) = 1. \tag{21}$$

In order to quantify the strength of the phase transition we determine several quantities. These are evaluated at the end of the phase transition, when most cosmological processes such as baryogenesis and gravitational wave production take place. The first quantity is the ratio between the Higgs VEV and the temperature, $\phi(T)/T$. This ratio is important for baryogenesis, since suppression of washout effects by sphalerons [11] requires $\phi(T)/T \gtrsim 1.0$ in the standard model. We do not expect this bound to be much different in the present model, since the sphaleron energy is dominated by the contributions from the gauge field configurations excited in the sphaleron rather than the scalar ones [12]. The second quantity is the duration of the phase transition $1/\beta$, which is given by

$$\frac{\beta}{H} = T\frac{d}{dT}\left(\frac{S_3}{T}\right). \tag{22}$$

The last quantity we are interested in is the latent heat

$$\epsilon = T\frac{d(V(\phi) - V(0))}{dT} - V(\phi) + V(0). \tag{23}$$

The latent heat is usually normalized to the energy density of the radiation in the plasma, through the dimensionless parameter α

$$\alpha = \frac{\epsilon}{\rho_{\rm rad}} = \frac{30\epsilon}{\pi^2 g_* T^4}. \tag{24}$$

The quantities α and β, as well as the bubble velocity v_b, are the key parameters that govern gravitational wave production (discussed in a later section).

For our numerical examples we take, as in Ref. [2], a number of scalars $N_S = 12$ with universal couplings to the Higgs, $\zeta_i = \zeta$, and no explicit mass terms, $m_{S_i} = 0$. The results for the electroweak phase transition parameters listed above, as functions of ζ and for several values of the Higgs mass m_H (consistent with electroweak breaking conditions), are plotted in Figs. 1–3. For small values of ζ, the phase transition is SM-like and therefore it is of second order or a crossover. As expected, the phase transition is in general stronger for larger values of ζ and smaller Higgs masses. The latent heat (as described by α) and the strength of the transition [as measured by $\phi(T)/T$] are both quickly increasing with ζ and larger for smaller m_H (see Fig. 1). In the figures we mark the conformal case with a cross and we see that, even in this case, the model shows a first-order phase transition strong enough to allow for electroweak baryogenesis (see Fig. 3). To the right of that conformal point the Higgs potential of the model has a barrier separating the symmetric and broken phases even at $T = 0$. For too large values of ζ this barrier becomes too high and tunneling by thermal fluctuations is not efficient to trigger the electroweak phase transition. Note how the time of the transition, $1/\beta$, gets larger and larger with increasing ζ. Eventually no thermal transition will occur beyond a critical point ζ_c and one would get stuck in the symmetric minimum (see below).

Finally we point out that in the present model a strong first-order phase transition does not necessarily imply a very large deviation of the cubic Higgs coupling from its SM value. Independently of the value of the Higgs mass, a

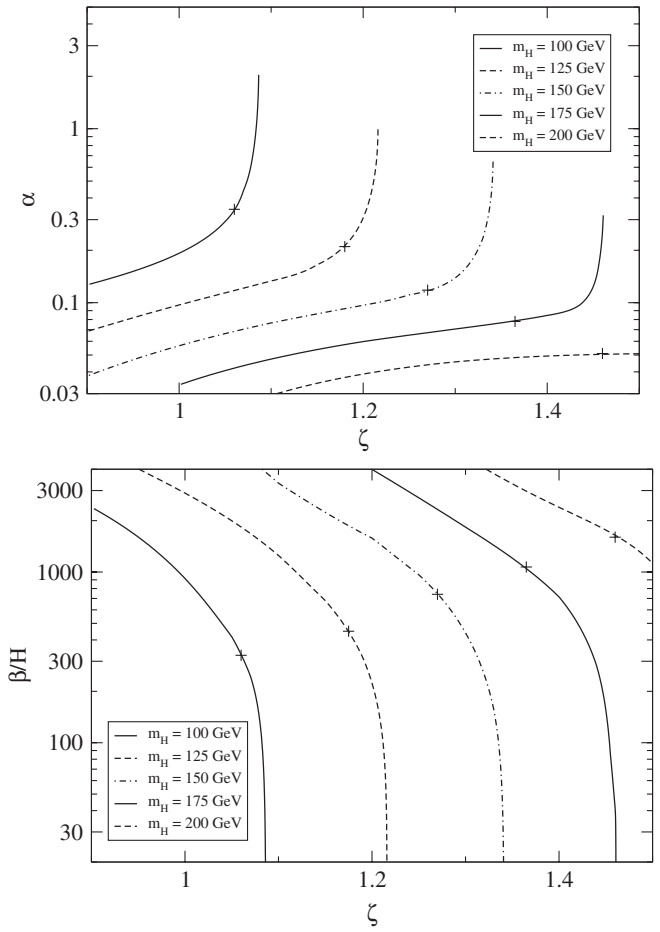

FIG. 1. The parameters α and β characterizing the electroweak phase transition as functions of ζ for several Higgs masses. A universal coupling ζ and $N_S = 12$ scalar fields have been used. The crosses mark the conformal case.

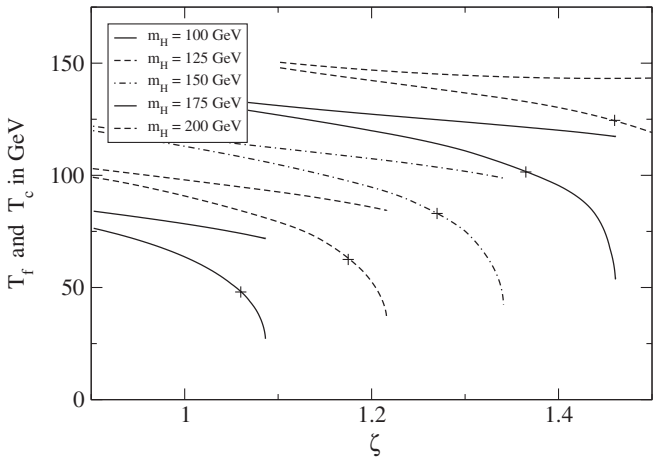

FIG. 2. Same as in Fig. 1 but for the critical temperature for vacuum degeneracy T_c (upper curve) and the temperature at the end of the phase transition T_f (lower curve).

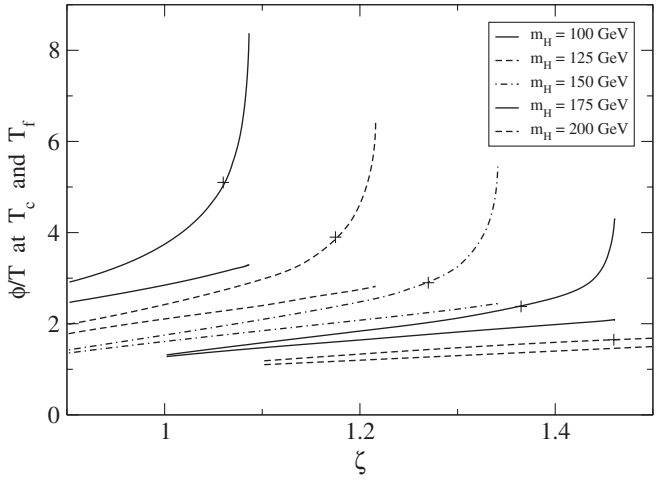

FIG. 3. Same as in Fig. 1 for the ratio ϕ/T at the critical temperature T_c (lower curve) and at the end of the phase transition, when the temperature is T_f (upper curve).

phase transition that is strong enough for the suppression of sphaleron processes, $\phi(T)/T \gtrsim 1.0$, is possible for deviations of the cubic coupling as small as 15%, as can be seen from Fig. 4.

B. Low-scale inflation

Every time a relatively strong first-order phase transition occurs during the evolution of the Universe the plasma undergoes a stage of large overcooling. This means that the energy finally released as latent heat is large compared to the thermal energy stored in the plasma. In this context it is worthwhile to ask whether during the stage of overcooling the expansion of the Universe is significantly accelerated due to the dominance of the vacuum energy, i.e. whether

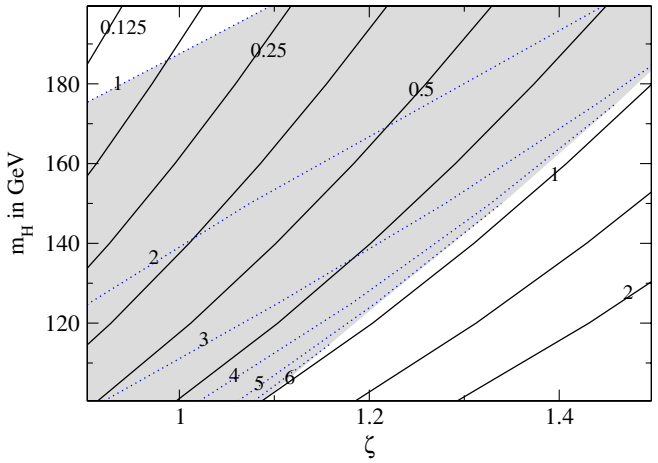

FIG. 4 (color online). The deviation of the cubic Higgs coupling from its value in the standard model (solid lines). The shaded region corresponds to a strong first-order phase transition: the dotted lines are labeled by the corresponding value of ϕ/T_f.

inflation occurs. This might be interesting in order to connect the predictions of inflation to low energy physics, but also for more exotic scenarios like cold electroweak baryogenesis [13,14].

However, if inflation takes place at electroweak scales the problem on whether this scenario allows for a graceful exit arises. It is well known that a realistic first-order phase transition cannot proceed arbitrarily slow, since percolation requires the decay rate of the vacuum to become rather large at a certain temperature [15]. This severely constrains the prospects of low-scale inflation in such scenarios. We will now analyze the two possible scenarios.

The first scenario is that inflation ends by thermal tunneling [10]. In this case a substantial amount of inflation is hardly achieved as can be seen as follows. Suppose that nucleation takes place after N_e e-folds of inflation. In this case the nucleation temperature, T_n, will be very low compared to the temperature of degenerate vacua $T_c \lesssim v$

$$N_e = \log(T_c/T_n) \lesssim \log(v/T_n). \tag{25}$$

The Higgs VEV will have to remain stuck in the symmetric phase down to very small temperatures and the energy density will be dominated by the vacuum energy, $V(0)$, rather than by the thermal energy of the plasma. Roughly speaking, the vacuum energy is related to the temperature of degenerate vacua, such that the Hubble parameter is

$$H^2 \propto \frac{V(0)}{M_{\rm Pl}^2} \propto \frac{v^2 T_c^2}{M_{\rm Pl}^2}. \tag{26}$$

Imposing that the thermal decay rate at T_n is larger than the Hubble rate we get the condition

$$\frac{S_3(T_n)}{T_n} \lesssim 4\log\left(\frac{T_n}{H}\right) \simeq 142 + 4\log\left(\frac{T_n}{T_c}\right) = 142 - 4N_e \lesssim 142. \tag{27}$$

In this regime of very small nucleation temperature the three-dimensional action (that increases with temperature) has therefore to be much smaller than the electroweak scale:

$$S_3(T_n \ll v) \lesssim 142 T_n \simeq 142 T_c e^{-N_e} \ll v. \tag{28}$$

This requires the potential barrier at zero temperature to be very small and we are thus led to the parameter region near the conformal case (in the conformal limit the barrier and the three-dimensional tunnel action vanish). In particular, the parameter ζ cannot be much larger than in the conformal case. However we know that near the conformal case the Higgs VEV does not get stuck at the origin: in fact the phase transition occurs already at temperatures of electroweak size, as can be seen in Fig. 2.

The fact that $T_n \lesssim T_c$ in the conformal case can be understood as follows: The potential difference between the symmetric minimum and the broken minimum is in this case given by

$$V(v) \simeq \frac{m_H^2 v^2}{16}. \tag{29}$$

The comparison of Eq. (29) with the thermal contributions to the potential in Eq. (9) shows that the temperature T_c where the two minima are degenerate is of order of the Higgs mass. At the same time, the potential barrier between the minima is absent at zero temperature, arising solely by temperature effects. Therefore one expects that the phase transition takes place with a nucleation temperature T_n of order T_c. In particular, the temperatures T_n and T_c increase with increasing Higgs mass. All this agrees with the numerical results as shown in Fig. 2.

The second scenario is that the minimum at the origin does not decay by thermal fluctuations but rather through vacuum (quantum) tunneling [8]. Instead of Eq. (14), the tunneling rate for vacuum decay is given by

$$\Gamma \simeq \kappa_4 v^4 \exp[-S_4(T)], \tag{30}$$

where S_4 denotes the four-dimensional tunnel action [16] and $\kappa_4 = [S_4/(2\pi)]^2$. Also in this case the first-order phase transition should not proceed arbitrarily slow and percolation requires, similar to Eq. (18),

$$S_4(T_n) \simeq 4\log\left(\frac{v}{H}\right) \simeq 142 - 8\log\left(\frac{v}{T_n}\right). \tag{31}$$

In order to assure that the minimum at the origin does not decay by thermal fluctuations, we should be in a parameter region in which there is a sufficiently large barrier at zero T. This occurs when ζ is larger than its conformal value that can be read off (for a fixed Higgs mass) from Fig. 1. Numerically, one finds that in this large-barrier regime the quantum tunneling probability is suppressed ($S_4 \gtrsim 200$), such that quantum tunneling cannot provide a graceful exit.

This result was to be expected, since to obtain stability under thermal fluctuations, a barrier comparable to the difference in vacuum energy is mandatory. In such a regime the tunneling actions can be calculated using the thin-wall approximation and one finds the scaling behavior

$$S_3(T) \propto v\left[\frac{v^4}{V(T,v)}\right]^2, \qquad S_4(T) \propto \left[\frac{v^4}{V(T,v)}\right]^3. \tag{32}$$

This shows that, for $V(v) \simeq v^4$, quantum tunneling is typically as unlikely as tunneling by thermal fluctuations.

As a conclusion we see that, in general, low-scale inflation with only one field seems to require two amply separate scales as, for example, in the case discussed in Ref. [17].

To end this section we show in Fig. 5 the typical behavior of the tunneling actions, S_3/T and S_4, as functions of the temperature for $M_H = 125$ GeV and two choices of ζ. For $\zeta = 1.2$, S_3/T gets eventually below the critical nucleation value $\sim$142 (horizontal line), and the electroweak phase transition takes place. For $\zeta = 1.25$ no satisfactory

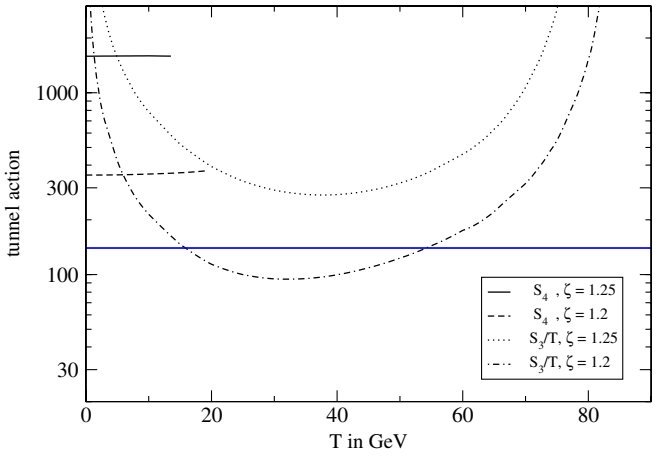

FIG. 5 (color online). Tunneling actions, S_3/T and S_4, as a function of temperature for $M_H = 125$ GeV and two different values of the coupling ζ as indicated. The curves for S_4 are stopped when the four-dimensional bounce ceases to be reliable.

transition would occur as the strong suppression will hinder percolation.

C. Bubble wall velocities

During a strongly first-order phase transition the wall velocity of the expanding nucleated bubbles is an important parameter. For example, the standard picture of electroweak baryogenesis is based on the diffusion of charge asymmetries into the unbroken phase in front of the wall. This effect is strongly suppressed if the wall expansion is supersonic, making electroweak baryogenesis implausible. On the other hand, gravitational wave production requires large wall velocities. Hence, baryogenesis and gravitational wave production at electroweak scales seem to be mutually exclusive [18].

The wall velocity does not only depend on the thermodynamical characteristics of the phase transition, but also on the particle content of the plasma. In particular, bosonic degrees of freedom that are massless before the phase transition but become heavy due to a strong coupling to the Higgs VEV exert a strong friction force on the wall [19–21]. In this way the presence of many hidden-sector scalars leads to subsonic wall velocities and the phase transition proceeds by *deflagration*. Following the arguments of Ref. [21], in the present case the friction is dominated by the scalars and is given by

$$\eta \approx \frac{N_S m_D^2 T}{16\pi L} \log(M_S L), \tag{33}$$

where $L \approx 1/T$ denotes the thickness of the bubble wall during the phase transition and $m_D^2 = \frac{1}{3}\zeta^2 T^2$ is the squared Debye mass of the hidden-sector scalars.

The expansion of the bubbles is driven by the pressure produced by the latent heat, $p = \epsilon/3$. If the friction forces are large, $\eta \gg p$, the wall velocity can be estimated to be $v_b = p/\eta$. Comparison with Eq. (33) shows that this is the case if the phase transition is weak, in the sense that $\alpha \ll (6 \times 10^{-3})\sum_i \zeta_i^2$.

In the opposite regime, in which friction effects from the plasma on the bubble wall are negligible, one expects the phase transition to proceed by *detonation*. In this case the bubble wall velocity can be determined by a self-consistent calculation that leads to supersonic wall velocities [22]. The wall velocity is then approximately given by

$$v_b = \frac{\sqrt{1/3} + \sqrt{\alpha^2 + 2\alpha/3}}{1 + \alpha}, \tag{34}$$

where α is the latent heat normalized to the energy density of the plasma as given in Eq. (24). In fact, this value for the wall velocity is only an upper bound, since a larger class of detonation solutions is known to exist [23], but we use nevertheless this formula in the analysis of gravitational wave production.

The results presented in Fig. 1 show that in principle both possibilities can occur in hidden-sector scalar extensions of the SM without significant tuning.

D. Gravitational waves

Another smoking-gun signal of a cosmological first-order phase transition is gravitational wave (GW) radiation. When the Higgs bubbles nucleate and expand, a portion of the latent heat is transformed into kinetic energy of the Higgs field and also into bulk motion of the plasma that follows the passing bubble wall profile. When the bubbles finally percolate and collide, this energy is partially released into gravitational waves [24–27]. Surprisingly, the only parameters that enter into the analysis of the gravitational wave radiation by collisions are the latent heat normalized to the radiation energy α, the wall velocity of the bubbles v_b, and the duration of the phase transition $1/\beta$.

In principle, there might be additional mechanisms of GW production, as e.g. turbulence in the plasma [28] and/or magnetic fields [29]. However, for very strong phase transitions, the peak frequency of the GW spectrum is shifted to lower frequencies and mostly the high frequency part of the GW spectrum lies in the range of best experimental sensitivity of the planned space-based experiments. The contributions from bubble collisions usually dominate for $f \gg f_{\text{peak}}$, such that at the frequency of best sensitivity of LISA or BBO, it suffices to consider the contributions from collisions. A more complete discussion of these issues can be found in Refs. [18,30,31].

In the following we summarize the formulas for GW production by bubble collisions as recently presented in Ref. [27]. The peak frequency is given by

$$f_{\text{peak}} \simeq 10.2 \times 10^{-3}\ \text{mHz}\left(\frac{\beta}{H}\right)\left(\frac{T_f}{100\ \text{GeV}}\right)\left(\frac{1.0}{1.8 + v_b^2}\right), \tag{35}$$

whereas the energy density in GWs amounts to

$$h^2\Omega_{\rm peak} = 1.84\times 10^{-6}\kappa^2\frac{H^2}{\beta^2}\left(\frac{\alpha}{1+\alpha}\right)^2\frac{v_b^3}{0.42+v_b^2}. \quad (36)$$

The efficiency factor κ indicates the fraction of latent heat that is transformed into bulk motion of the plasma and finally into gravitational waves. It is given by [24]

$$\kappa = \frac{1}{1+0.715\alpha}\left[0.715\alpha+\frac{4}{27}\sqrt{\frac{3\alpha}{2}}\right]. \quad (37)$$

The best sensitivity of BBO (LISA) is at $f = 100$ mHz ($f = 1$ mHz) expected to be $h^2\Omega = 10^{-17}$ ($h^2\Omega = 10^{-11}$). Considering that the GW spectrum from collisions scales approximately as $h^2\Omega \propto 1/f$ for large frequencies [27], one obtains for BBO a signal to sensitivity ratio

$$1.87\times 10^7\kappa^2\left(\frac{\alpha}{\alpha+1}\right)^2\left(\frac{T_f}{100\ \text{GeV}}\right)\left(\frac{H}{\beta}\right)\times\left(\frac{v_b^3}{0.76+2.22v_b^2+v_b^4}\right), \quad (38)$$

and for LISA a value that is smaller by four orders of magnitude.

Comparison with the parameters of the phase transition in Fig. 1 shows that in the present model a signal that is detectable by BBO is feasible, if the parameter ζ is rather close to the critical point ζ_c beyond which no thermal tunneling occurs, requiring a tuning in ζ at the percent level. For example, the parameters

$$\alpha = 0.2, \qquad \beta/H = 200, \qquad T_f = 50\ \text{GeV}, \quad (39)$$

lead to [using (34) and (37)]

$$v_b = 0.83, \qquad \kappa = 0.20, \quad (40)$$

and to a signal to sensitivity ratio of $O(10)$. On the other hand, no observable traces from the electroweak phase transition are expected at LISA in the present model.

E. Dark matter

In this section we investigate if the new scalar degrees of freedom constitute a viable dark matter candidate. For simplicity we consider only one hidden-sector scalar as the generalization to several scalars is straightforward. Singlet dark matter has already been extensively discussed in the literature (see e.g. Refs. [32–34]). Here we focus on two aspects. First, we discuss if the same scalar species might be responsible both for a strong phase transition and for dark matter (Ref. [35] addresses the same question in a different extension of the Higgs sector). Second, we focus on the classically conformal case, in which the scalar has no explicit mass term.

The scalar has to be stable to constitute a viable dark matter candidate. This is achieved by the choice of the potential in Eq. (1), since the scalars are protected from decay by a Z_2 symmetry. In particular we assume that this symmetry is not spontaneously broken. Nevertheless the scalars annihilate and the particle density of the scalar obeys the Boltzmann equation [33]

$$\frac{dn_S}{dt} = -3Hn_S - \langle\sigma_{\rm ann}v\rangle(n_S^2 - n_{S,\rm eq}^2), \quad (41)$$

where the equilibrium distribution is given by

$$n_{S,\rm eq} = T^3\left(\frac{M_S}{2\pi T}\right)^{3/2}e^{-M_S/T}, \quad (42)$$

and H denotes the Hubble parameter as given in Eq. (16). Rescaling the distribution functions, $f = n/T^3$, one obtains the equation

$$\frac{df_S}{dT} = \frac{\langle\sigma_{\rm ann}v\rangle}{H/T^2}(f_S^2 - f_{S,\rm eq}^2). \quad (43)$$

The contributions to $\langle\sigma_{\rm ann}v\rangle$ from annihilation to pairs of Higgs, W, Z bosons and SM fermions are, respectively, given by

$$\begin{aligned}\langle\sigma_{\rm ann}v\rangle =& \frac{\zeta^4}{16\pi M_S^2}\left(1-\frac{M_H^2}{M_S^2}\right)^{1/2}\left\{1+\frac{3M_H^2}{D_h}(8M_S^2+M_H^2)\right.\\ &+\frac{8\zeta^2v^2}{D_S}(M_H^2+2\zeta^2v^2-2M_S^2)-\left(\frac{3M_H^2}{D_h}\right)\left(\frac{8\zeta^2v^2}{D_S}\right)\\ &\left.\times[(4M_S^2-M_H^2)(2M_S^2-M_H^2)-M_HM_S\Gamma_H\Gamma_S]\right\}\\ &+\frac{\zeta^4M_W^4}{2\pi M_S^2D_h}\left(1-\frac{M_W^2}{M_S^2}\right)^{1/2}\left[2+\left(1-2\frac{M_S^2}{M_W^2}\right)^2\right]\\ &+\frac{1}{2}(M_W^2\to M_Z^2)+\sum_{\rm fermions}\frac{N_f\zeta^4M_f^2}{\pi D_h}\left(1-\frac{M_f^2}{M_S^2}\right)^{3/2},\end{aligned} \quad (44)$$

where

$$\begin{aligned}D_h &\equiv (4M_S^2 - M_H^2)^2 + M_H^2\Gamma_H^2,\\ D_S &\equiv (2M_S^2 - M_H^2)^2 + M_S^2\Gamma_S^2,\end{aligned} \quad (45)$$

$\Gamma_H \approx 8\times 10^{-5}M_H$ is the decay width of the Higgs particle in the SM and Γ_S that of the hidden scalars. Finally, $N_f = 1(3)$ for leptons (quarks).

An approximate solution to this equation was given in Ref. [36]. The scalar freeze-out temperature $\hat{T}$ is given by

$$\frac{M_S}{\hat{T}} = \log\left(\frac{M_S\langle\sigma_{\rm ann}v\rangle}{H/\hat{T}^2}\right)+\frac{1}{2}\log\left(\frac{8\pi^3\hat{T}}{M_S}\right), \quad (46)$$

and typically one finds $M_S \approx (15\text{–}25)\hat{T}$. The final particle density is

$$f(T \ll M_S) \approx \frac{H/\hat{T}^2}{\hat{T}\langle\sigma_{\rm ann}v\rangle}. \quad (47)$$

At present, $T = T_\gamma$, the total energy density in scalars is

$$\Omega_{\rm DM} = \frac{2}{g_*}\frac{M_S n_S(T_\gamma)}{\rho_{\rm crit}} = \frac{2}{g_*}\frac{H/T^2}{\hat{T}\langle\sigma_{\rm ann}v\rangle}\frac{M_S T_\gamma^3}{\rho_{\rm crit}}, \qquad (48)$$

where $\rho_{\rm crit}$ denotes the critical energy density of the Universe at present.

The dependence of $\Omega_{\rm DM}$ on the scalar mass for fixed coupling ζ is plotted in Fig. 6. Notice that we only plotted the dark matter density for scalar masses that are larger than ζv and hence correspond to a positive mass term in the Lagrangian (according to $M_S^2 = \zeta^2 v^2 + m_S^2$).

Besides a logarithmic dependence on the freeze-out temperature, the dark matter density scales for large masses as $\Omega_{\rm DM} \propto M_S^2/\zeta^4$. Notice that for $2M_S \approx M_H$ most annihilation channels are enhanced and the scalar contribution to dark matter is suppressed. Finally, the annihilation cross section drops considerably below the W-boson threshold, $M_S < M_W$, since if the scalar is light it mostly annihilates into bottom/antibottom pairs, which is suppressed by the bottom-quark Yukawa coupling. This leads to an increase of the dark matter density below the W-boson threshold. Notice that taking temperature effects into account, one expects that the annihilation cross section changes less drastically when the scalar mass is varied. In particular the enhancement close to the Higgs mass is expected to be less prominent. Likewise, the drop below the W-boson threshold proceeds in an interval of width $\Delta M_S \approx T$.

Therefore, we see that there are two valid regimes of scalar dark matter. The first option is to increase the scalar mass term m_S, while keeping the coupling ζ fixed. However, even in the case of a rather large number of scalars $N_S = 12$, this requires scalar masses of order TeV and such scalars cannot be responsible for a strong phase transition. Alternatively, the scalar could be rather light, with $M_S \lesssim M_W$, and weakly coupled, such that its annihilation is suppressed. Also in this case, the impact of the scalars on the phase transition is small.

Finally, consider a model without an explicit singlet mass term in the Lagrangian. In Fig. 7 the dark matter density is plotted as a function of ζ for $M_S = \zeta v$ and for two different values of the Higgs mass. The predicted dark matter density typically surpasses the observed one below the W-boson threshold. Besides, in the case that the Higgs boson is lighter than two W bosons, the resonant enhancement in the decay channel can lead to two additional viable values for the parameter ζ that reproduce the observed dark matter density. Again, such weakly coupled scalars cannot increase the strength of the phase transition considerably. In particular, a classically conformal model requires several additional, strongly coupled scalars to surpass the current bounds on the Higgs mass, see Fig. 1.

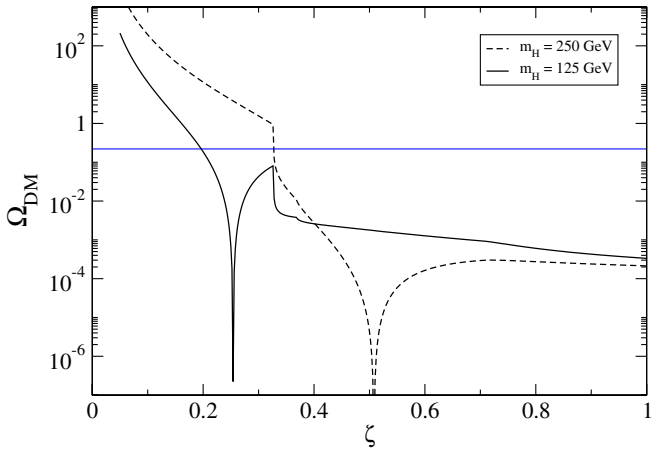

FIG. 7 (color online). Dark matter density of a single hidden scalar as a function of the coupling ζ in the case $M_S = \zeta v$ and for two different values of the Higgs mass.

In conclusion, if extra scalar degrees of freedom are responsible for a strong electroweak first-order phase transition, as well as for dark matter, it seems that either the coupling constants ζ_i or the mass terms $m_{S,i}$ are nonuniversal. Scalar dark matter requires either a scalar with a rather large mass $M_S \approx$ TeV, or a rather weak coupling $\zeta \approx M_W/v$. However, both types of scalars cannot contribute significantly to the strength of the phase transition. Hence, the existence of both features in a universal scalar framework would require a very large number of scalars, which we estimate to be $N_S \gtrsim 50$.

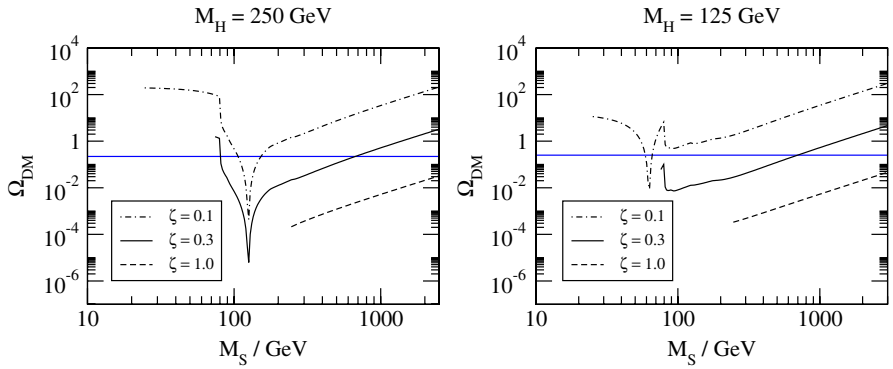

FIG. 6 (color online). Dark matter density of a single hidden scalar (for two different Higgs masses as indicated) as a function of the scalar mass M_S and different values for its coupling to the Higgs, ζ.

IV. CONCLUSIONS

We have studied several cosmological implications of standard model extensions with hidden-sector scalars. In particular, we strengthen the results of [2] finding that in models with a moderate number of hidden-sector scalars, $N_S \approx 12$, the electroweak phase transition is generically of first order as long as the Higgs mass is not much larger than the electroweak scale and the coupling to the hidden sector is substantial, $\zeta \gtrsim 0.9$. An interesting feature of the model is that this property persists even if the theory is classically conformal invariant and the electroweak scale is induced by dimensional transmutation. This was already emphasized in Ref. [2]. We find that the phase transition is in a large portion of the parameter space strong enough to suppress the sphaleron process after the phase transition, $\phi/T \gtrsim 1.0$ as required by electroweak baryogenesis. Besides, we find that sizable production of gravitational radiation requires a tuning of the parameters at the percent level.

Besides a strong first-order phase transition, viable electroweak baryogenesis requires sizable *CP* violation. Electroweak baryogenesis in non-SUSY models typically utilizes a Higgs VEV that has a changing complex phase during the phase transition. One useful ingredient hence seems to be to complexify the present scalars and to allow for scalar VEVs, but still this would not induce a change in the complex phase of the Higgs VEV such that the introduction of a second Higgs doublet seems unavoidable. Alternatively, one can introduce an additional source of *CP* violation in the quark sector (see e.g. Ref. [37]) but undoubtedly *CP* violation arising from the hidden sector would be much more appealing in our model.

Concerning dark matter, we find that the abundance required by the concordance model can be provided by hidden-sector scalars in two different regimes. In the first, the hidden-sector scalars have moderate couplings but large masses $M_S \gtrsim 1$ TeV. In the second, the hidden-sector scalars are rather light, $M_S \lesssim M_W$. In this case, the scalars cannot annihilate into W bosons, which greatly enhances the dark matter abundance. Notice that this scenario is compatible with scalars that obtain their mass solely by electroweak symmetry breaking. Nevertheless, neither type of scalar can contribute significantly to the strength of the phase transition, such that a viable dark matter candidate cannot substantially improve the prospects of electroweak baryogenesis compared to the SM. Hence, a simultaneous solution of the dark matter and baryogenesis problems of the standard model close to electroweak scales either requires a large number of scalars (in which case we found $N_S \gtrsim 50$), or several types of scalars in the hidden sector with nonuniform masses and/or couplings to the Higgs sector.

ACKNOWLEDGMENTS

J. R. E. thanks A. Casas, A. Riotto, and G. Servant for discussions. Work was supported in part by the European Commission under the European Union through the Marie Curie Research and Training Networks ''Quest for Unification'' (No. MRTN-CT-2004-503369) and ''UniverseNet'' (No. MRTN-CT-2006-035863); by a Comunidad de Madrid project (No. P-ESP-00346); and by CICYT, Spain, under Contracts No. FPA 2007-60252 and No. FPA 2005-02211. T. K. is supported by the EU FP6 Marie Curie Research and Training Network ''UniverseNet'' (No. MRTN-CT-2006-035863).

[1] R. Schabinger and J. D. Wells, Phys. Rev. D **72**, 093007 (2005); B. Patt and F. Wilczek, arXiv:hep-ph/0605188; M. Bowen, Y. Cui, and J. D. Wells, J. High Energy Phys. 03 (2007) 036.
[2] J. R. Espinosa and M. Quirós, Phys. Rev. D **76**, 076004 (2007).
[3] S. R. Coleman and E. Weinberg, Phys. Rev. D **7**, 1888 (1973).
[4] R. Jackiw, Phys. Rev. D **9**, 1686 (1974).
[5] In this case it is obvious that the one-loop Higgs mass differs significantly from its tree-level value $m_H^2 = 3\lambda v^2$. Similarly the Goldstone boson is massless at one loop unlike the tree-level result $m_G^2 = \lambda v^2$. This discrepancy between the tree-level and one-loop masses does also appear in the nonconformal case. It usually does not constitute a significant complication, since the loop contributions of the Higgs and Goldstone bosons are small.
[6] See e.g. J. R. Espinosa and R. J. Zhang, Nucl. Phys. **B586**, 3 (2000).
[7] A. Noble and M. Perelstein, Phys. Rev. D **78**, 063518 (2008).
[8] S. R. Coleman, Phys. Rev. D **15**, 2929 (1977); **16**, 1248(E) (1977).
[9] C. G. Callan and S. R. Coleman, Phys. Rev. D **16**, 1762 (1977).
[10] A. D. Linde, Phys. Lett. B **100**, 37 (1981); Nucl. Phys. **B216**, 421 (1983); **B223**, 544(E) (1983).
[11] G. R. Farrar and M. E. Shaposhnikov, Phys. Rev. D **50**, 774 (1994).
[12] F. R. Klinkhamer and N. S. Manton, Phys. Rev. D **30**, 2212 (1984).
[13] J. García-Bellido, D. Y. Grigoriev, A. Kusenko, and M. E. Shaposhnikov, Phys. Rev. D **60**, 123504 (1999).
[14] A. Tranberg and J. Smit, J. High Energy Phys. 11 (2003) 016.
[15] A. H. Guth and E. J. Weinberg, Nucl. Phys. **B212**, 321

(1983).
[16] The four-dimensional bounce solution can be trusted as long as its radius is smaller than $1/T$. Above some (small) temperature the three-dimensional bounce solution should be considered instead.
[17] G. Nardini, M. Quirós, and A. Wulzer, J. High Energy Phys. 09 (2007) 077.
[18] S. J. Huber and T. Konstandin, J. Cosmol. Astropart. Phys. 05 (2008) 017.
[19] G. D. Moore and T. Prokopec, Phys. Rev. Lett. **75**, 777 (1995).
[20] G. D. Moore and T. Prokopec, Phys. Rev. D **52**, 7182 (1995).
[21] G. D. Moore, J. High Energy Phys. 03 (2000) 006.
[22] P. J. Steinhardt, Phys. Rev. D **25**, 2074 (1982).
[23] M. Laine, Phys. Rev. D **49**, 3847 (1994).
[24] M. Kamionkowski, A. Kosowsky, and M. S. Turner, Phys. Rev. D **49**, 2837 (1994).
[25] R. Apreda, M. Maggiore, A. Nicolis, and A. Riotto, Nucl. Phys. **B631**, 342 (2002).
[26] C. Caprini, R. Durrer, and G. Servant, Phys. Rev. D **77**, 124015 (2008).
[27] S. J. Huber and T. Konstandin, J. Cosmol. Astropart. Phys. 09 (2008) 022.
[28] A. Kosowsky, A. Mack, and T. Kahniashvili, Phys. Rev. D **66**, 024030 (2002); A. D. Dolgov, D. Grasso, and A. Nicolis, Phys. Rev. D **66**, 103505 (2002); G. Gogoberidze, T. Kahniashvili, and A. Kosowsky, Phys. Rev. D **76**, 083002 (2007); T. Kahniashvili, G. Gogoberidze, and B. Ratra, Phys. Rev. Lett. **100**, 231301 (2008); A. Megevand, Phys. Rev. D **78**, 084003 (2008).
[29] C. Caprini and R. Durrer, Phys. Rev. D **74**, 063521 (2006); E. Fenu and R. Durrer, arXiv:astro-ph/0809.1383.
[30] A. Nicolis, Classical Quantum Gravity **21**, L27 (2004).
[31] C. Grojean and G. Servant, Phys. Rev. D **75**, 043507 (2007).
[32] V. Silveira and A. Zee, Phys. Lett. B **161**, 136 (1985).
[33] J. McDonald, Phys. Rev. D **50**, 3637 (1994).
[34] C. P. Burgess, M. Pospelov, and T. ter Veldhuis, Nucl. Phys. **B619**, 709 (2001).
[35] T. Hambye and M. H. G. Tytgat, Phys. Lett. B **659**, 651 (2008).
[36] B. W. Lee and S. Weinberg, Phys. Rev. Lett. **39**, 165 (1977).
[37] D. Bodeker, L. Fromme, S. J.Huber, and M. Seniuch, J. High Energy Phys. 02 (2005) 026.